



Short communication

Development of fluorinated methoxylated chalcones as selective monoamine oxidase-B inhibitors: Synthesis, biochemistry and molecular docking studies



Bijo Mathew^{a,*}, Githa Elizabeth Mathew^b, Gülberk Uçar^c, Ipek Baysal^c, Jerad Suresh^d, Jobin Kunjumon Vilapurathu^a, Aneesh Prakasan^b, Jeethu Kuruppath Suresh^b, Anjana Thomas^b

^a Division of Drug Design and Medicinal Chemistry Research Lab, Department of Pharmaceutical Chemistry, Grace College of Pharmacy, Palakkad 678004, Kerala, India

^b Department of Pharmacology, Grace College of Pharmacy, Palakkad 678004, Kerala, India

^c Department of Biochemistry, Faculty of Pharmacy, Hacettepe University, 06100 Sıhhiye, Ankara, Turkey

^d Department of Pharmaceutical Chemistry, Madras Medical College, Chennai 600004, India

ARTICLE INFO

Article history:

Received 9 June 2015

Revised 6 July 2015

Accepted 7 July 2015

Available online 9 July 2015

Keywords:

Methoxylated chalcone

MAO-A

MAO-B

Molecular docking

ABSTRACT

A series of methoxylated chalcones with fluoro and trifluoromethyl derivatives were synthesized and investigated for their ability to inhibit human monoamine oxidase A and B. The chemical structures of the compounds have been characterized by means of their ¹H NMR, ¹³C NMR, Mass spectroscopic data and elemental analysis. The results demonstrate that these compounds are reversible and selective MAO-B inhibitors with a competitive mode of inhibition. The most potent compound (2*E*)-1-(4-methoxyphenyl)-3-[4-(trifluoromethyl)phenyl] prop-2-en-1-one showed the best activity and higher selectivity towards hMAO-B with *K_i* and SI values of 0.22 ± 0.01 μM and 0.05 comparable to that standard drug, Selegiline *K_i* and SI values were found as 0.33 ± 0.03 μM and 0.04, respectively. Molecular docking studies were carried out to further explain the *in vitro* results of the new compounds, and to identify the hypothetical binding mode for the compounds inside the inhibitor binding cavity of hMAO-B.

© 2015 Elsevier Inc. All rights reserved.

1. Introduction

Recognition of the catalytic site of monoamine oxidases (MAO) represents as promising targets for intervention in many amine oxidase-related disorders like depression and Parkinson's disease [1]. MAO inhibitors (MAOIs) are classified as reversible or irreversible, according to their interaction with the isoform. MAO irreversible inhibitors previously have been used as clinical drugs. However, this type of inhibition has been shown to induce cardiovascular toxic effects, mainly provoked by the inhibition of the peripheral MAO located in gut, liver and endothelium. On the other hand, competitive, reversible inhibitors have less influence in the enzyme recovery after withdrawal as the ingested tyramine is able to displace the inhibitor from the MAO active site and be metabolized in the normal way by a peripheral enzyme in the gut and liver [2]. Besides, the slow and variable enzyme recovery following the withdrawal of irreversible inhibitors is a disadvantage in clinical use, since the turnover rate for MAO biosynthesis in the human

brain seems to require about 40 days [3]. So, newly synthesized reversible MAO-A and B inhibitors may cause a great healing value in this prospect.

In neurodegenerative disorders, including Parkinson's and Alzheimer's diseases, MAO-B has been proposed to play a prominent role, though generating reactive oxygen species (ROS) in the oxidation of monoamine substrates. The oxidative pathway of ROS can precipitate neuronal death in neurodegenerative disorders [4]. Inhibitors of MAO with selectivity and specificity of MAO type B prolong the activity of both endogenous and exogenously derived dopamine, making them an option either as monotherapy in early Parkinson's disease or as adjuvant therapy in patients treated with levodopa who are experiencing motor complications [5]. Thus the objective of our research program is to develop some selective and potent MAO-B inhibitors from therapeutically known scaffold.

Chalcones, three-carbon consists of α, β-unsaturated carbonyl system and are considered to be precursors of flavonoids and iso-flavonoids [6]. The competence of chalcone scaffolds to work along the central nervous system (CNS) is chiefly connected with its low polar surface area that can aid to thwart the blood brain barrier easily. This attribute is primarily made by the hydrophobic nature

* Corresponding author.

E-mail address: bijovilaventgu@gmail.com (B. Mathew).

of two aromatic nucleus of A and B between the open chain of α , β -unsaturated system [7]. The MAO inhibitory activities of chalcones have however, only been determined in a few instances for naturally occurring chalcones using rat, bovine and hamster monoamine oxidases, while some synthetic chalcone derivatives were screened against human MAO (hMAO) [8–16]. The gathered results suggested that chalcone derivatives displayed a selective inhibitory activity towards hMAO-B in the micro to nanomolar range. The presence of hydroxyl and methoxyl groups or two hydroxyl substituents in the ortho and para position of the A aromatic moiety as well as a chlorine atom in the para position of the B aromatic moiety is found to be a fundamental requisite for activity. On the other hand chalcones substituted with isoprenyloxy substructures have shown a lower activity [17].

So far many of fluorine and trifluoromethyl group containing CNS drugs has been applied in clinical practice, such as antidepressant-Fluoxetine, antipsychotic-Melperone, anti-anxiety agent-Halazepam, benzodiazepine antagonist-Flumazenil etc. (Fig. 1). Recently the cyclized product of dimethoxyl chalcone (2-aryl-4H-chromen-4-one) was found to be potent MAO-B inhibitor with K_i value for MAO-B of

$0.16 \pm 0.01 \mu\text{M}$ [18]. The present study aims to expand on the structure–activity relationships (SARs) of MAO inhibition by chalcone derivatives by synthesizing a series of fluorinated chalcones with methoxy substituted phenyl system. The information regarding the orientation of fluoro and trifluoromethyl groups in the B ring system of methoxylated chalcone and its effect of MAO inhibition is not explored so far. Para-methoxy acetophenone moiety was selected as starting reagent for the synthesis of various methoxylated chalcones. For this purpose, chalcones were obtained by a Claisen–Schmidt condensation between p-methoxy acetophenone and various substituted fluorine and trifluoromethyl benzaldehydes under basic conditions – Scheme 1 (Fig. 2).

2. Experimental

2.1. Materials and methods

All the fluorinated benzaldehydes were procured from Sigma–Aldrich USA. Melting points of all the synthesized derivatives were determined by open-capillary tube method and values

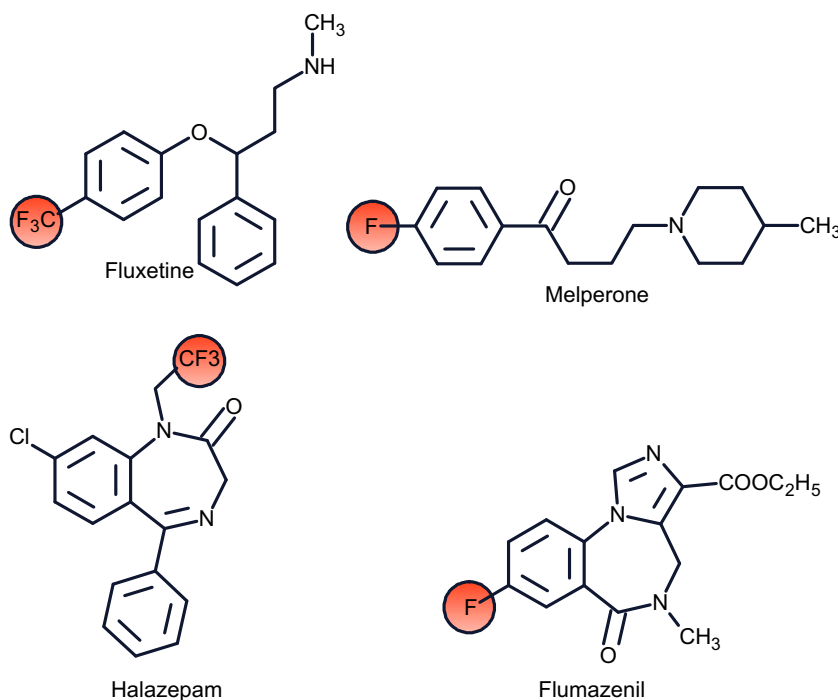


Fig. 1. Fluorinated CNS drugs.

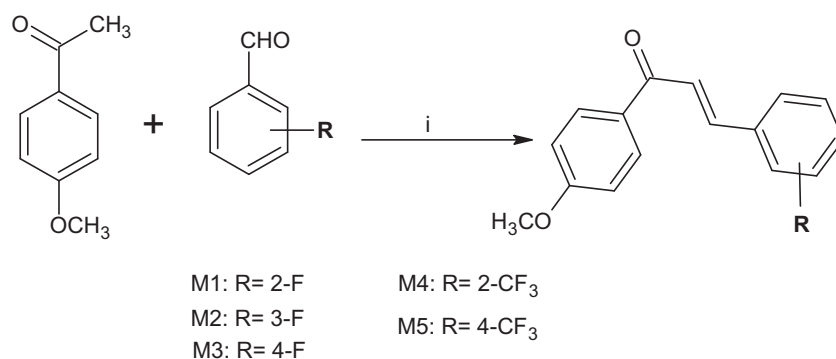


Fig. 2. Scheme 1 – Synthesis of fluorinated methoxylated chalcones; (i): Reagents and condition: $\text{C}_2\text{H}_5\text{OH}$, 40% KOH, stir. 4 h.

were uncorrected. Proton (^1H) and carbon (^{13}C) nuclear magnetic resonance (NMR) spectra were recorded on a Bruker Avance III 600 spectrometer at frequencies of 400 MHz and 100 MHz, respectively (Bruker, Karlsruhe, Germany). All NMR measurements were conducted in CDCl_3 , and the chemical shifts are reported in parts per million (δ) downfield from the signal of tetramethylsilane added to the deuterated solvent. Mass spectra were recorded on a JEOL GCmate mass spectrometer. Elemental analyses (C, H, N) were performed on a Leco CHNS 932 analyzer.

2.2. Chemistry

A mixture of 4-methoxy acetophenone (0.01 mol), fluorinated aldehyde (0.01 mol) and 40% aqueous potassium hydroxide (15 mL) in ethanol (30 mL) was stirred at room temperature for about 2–6 h. The resulting product was kept overnight in refrigerator. The solid separated was filtered, washed with water and recrystallized from ethanol.

2.2.1. (2E)-3-(2-fluorophenyl)-1-(4-methoxyphenyl) prop-2-en-1-one (**M1**)

Pale white solid, Yield: 88%, M.P: 89–91 °C. ^1H NMR (400 MHz, CDCl_3) δ ppm: 3.920 (s, 3H, 4'-OCH₃), 7.026–7.004 (d, 2H, J = 8.8 Hz, H₃' & H₅'), 7.128–7.110 (t, 1H, J = 7.2 Hz, H₅'), 7.150–7.143 (d, 1H, J = 2.8 Hz, H₃'), 7.398–7.379 (t, 1H, J = 7.6 Hz, H₄'), 7.418–7.398 (d, 1H, J = 8.0 Hz, H₆'), 7.577–7.538 (d, 1H, J = 15.6 Hz, CH _{α}), 7.792–7.753 (d, 1H, J = 15.6 Hz, CH _{β}), 8.077–8.055 (d, 2H, J = 8.8 Hz, H₄' & H₆'). ^{13}C NMR (100 MHz, CDCl_3) δ ppm: 188.33, 164.30, 163.61, 161.84, 142.43, 142.41, 137.45, 137.37, 130.87, 124.47, 124.44, 123.10, 117.23, 117.01, 113.93, 55.52. ESI-MS (m/z): calculated 256.271, observed 256.270 ($M + 1$)⁺. Anal. calcd. for C₁₆H₁₃FO₂: C, 74.99; H, 5.11. Found: C, 74.88; H, 5.21.

2.2.2. (2E)-3-(3-fluorophenyl)-1-(4-methoxyphenyl) prop-2-en-1-one (**M2**)

^1H NMR (400 MHz, CDCl_3) δ ppm: Pale white solid, Yield: 82%, M.P: 94–96 °C. 3.913 (s, 3H, 4'-OCH₃), 7.020–6.998 (d, 2H, J = 8.8 Hz, H₃' & H₅'), 7.149–7.127 (d, 1H, J = 8.8 Hz, H₄'), 7.234–7.215 (t, 1H, J = 7.6 Hz, H₆'), 7.386–7.369 (t, 1H, J = 6.8 Hz, H₅'), 7.681 (s, 1H, H₂'), 7.702–7.662 (d, 1H, J = 16.0 Hz, CH _{α}), 7.930–7.890 (d, 1H, J = 16.0 Hz, CH _{β}), 8.079–8.057 (d, 2H, J = 8.8 Hz, H₄' & H₆'). ^{13}C NMR (100 MHz, CDCl_3) δ ppm: 188.69, 163.54, 162.99, 160.48, 136.67, 131.61, 131.53, 130.96, 129.80, 124.62, 124.45, 123.28, 116.37, 116.16, 113.89, 55.49. ESI-MS (m/z): calculated 256.271, observed 256.260 ($M + 1$)⁺. Anal. calcd. for C₁₆H₁₃FO₂: C, 74.99; H, 5.11. Found: C, 74.91; H, 5.17.

2.2.3. (2E)-3-(4-fluorophenyl)-1-(4-methoxyphenyl) prop-2-en-1-one (**M3**)

Pale white solid, Yield: 90%, M.P: 106–108 °C. ^1H NMR (400 MHz, CDCl_3) δ ppm: 3.908 (s, 3H, 4'-OCH₃), 7.013–6.992 (d, 2H, J = 8.4 Hz, H₃' & H₅'), 7.143–7.722 (d, 2H, J = 8.4 Hz, H₃' & H₅'), 7.508–7.469 (d, 1H, J = 15.6 Hz, CH _{α}), 7.664–7.650 (d, 2H, J = 5.6 Hz, H₂' & H₅'), 7.801–7.862 (d, 1H, J = 15.6 Hz, CH _{β}), 8.065–8.043 (d, 2H, J = 8.8 Hz, H₄' & H₆'). ^{13}C NMR (100 MHz, CDCl_3) δ ppm: 188.46, 165.19, 163.50, 162.69, 142.60, 131.39, 131.36, 131.05, 130.79, 130.25, 121.66, 121.16, 116.16, 115.95, 113.98, 55.49. ESI-MS (m/z): calculated 256.271, observed 256.250 ($M + 1$)⁺. Anal. calcd. for C₁₆H₁₃FO₂: C, 74.99; H, 5.11. Found: C, 74.83; H, 5.16.

2.2.4. (2E)-1-(4-methoxyphenyl)-3-[2-(trifluoromethyl) phenyl] prop-2-en-1-one (**M4**)

Yellow solid, Yield: 87%, M.P: 78–80 °C. ^1H NMR (400 MHz, CDCl_3) δ ppm: 3.911 (s, 3H, 4'-OCH₃), 7.017–6.995 (d, 2H, J = 8.4 Hz, H₃' & H₅'), 7.472–7.433 (d, 1H, J = 15.6 Hz, CH _{α}),

7.533–7.514 (t, 1H, J = 7.6 Hz, H₅'), 7.621–7.602 (t, 1H, J = 7.6 Hz, H₄'), 7.754–7.734 (d, 1H, J = 8.0 Hz, H₃'), 7.853–7.834 (d, 1H, J = 7.6 Hz, H₆'), 8.061–8.039 (d, 2H, J = 8.8 Hz, H₄' & H₆'). 8.157–8.118 (d, 1H, J = 15.6 Hz, CH _{β}). ^{13}C NMR (100 MHz, CDCl_3) δ ppm: 188.47, 163.65, 139.31, 134.30, 132.06, 131.02, 130.60, 129.60, 128.99, 128.08, 127.96, 126.52, 125.15, 122.64, 119.91, 113.93, 55.50. ESI-MS (m/z): calculated 306.279, observed 306.240 ($M + 1$)⁺. Anal. calcd. for C₁₇H₁₃F₃O₂: C, 66.67; H, 4.28. Found: C, 66.78; H, 4.20.

2.2.5. (2E)-1-(4-methoxyphenyl)-3-[4-(trifluoromethyl) phenyl] prop-2-en-1-one (**M5**)

Pale yellow solid, Yield: 86%, M.P: 118–120 °C. 3.921 (s, 3H, 4'-OCH₃), 7.030–7.008 (d, 2H, J = 8.8 Hz, H₃' & H₅'), 7.648–7.609 (d, 1H, J = 15.6 Hz, CH _{α}), 7.699–7.679 (d, 2H, J = 8.0 Hz, H₃' & H₅'), 7.768–7.748 (d, 2H, J = 8.0 Hz, H₂' & H₅'), 7.837–7.798 (d, 1H, J = 15.6 Hz, CH _{β}), 8.083–8.061 (d, 2H, J = 8.8 Hz, H₄' & H₆'). ^{13}C NMR (100 MHz, CDCl_3) δ ppm: 188.18, 163.72, 141.87, 138.52, 131.87, 131.54, 130.92, 130.74, 128.41, 127.93, 125.88, 125.81, 125.23, 124.16, 122.52, 113.98, 55.52. ESI-MS (m/z): calculated 306.279, observed 306.270 ($M + 1$)⁺. Anal. calcd. for C₁₇H₁₃F₃O₂: C, 66.67; H, 4.28. Found: C, 66.56; H, 4.32.

2.3. Biochemistry

2.3.1. Chemicals

hMAO-A and hMAO-B (both recombinant, expressed in baculovirus-infected BTI insect cells), *R*-(–)-deprenyl hydrochloride (selegiline), moclobemide, resorufin, dimethyl sulfoxide (DMSO), and other chemicals were purchased from Sigma-Aldrich (Munich, Germany). The Amplex®-Red MAO assay kit (Cell Technology Inc., Mountain View, CA, USA) contained benzyamine, *p*-tyramine, clorgyline (MAO-A inhibitor), pargyline (MAO-B inhibitor), and horseradish peroxidase.

2.3.2. Determination of inhibitory activities of the fluorinated methoxylated chalcones on human MAO-A and B

The activities of hMAO-A and hMAO-B were determined using *p*-tyramine as common substrate and calculated as 161.50 ± 8.33 pmol/mg/min ($n = 3$) and 140.00 ± 7.99 pmol/mg/min ($n = 3$), respectively. The interactions of the synthesized fluorinated methoxylated chalcones with hMAO isoforms were determined by a fluorimetric method described and modified previously [19–21]. Study medium contained 0.1 mL of sodium phosphate buffer (0.05 M, pH 7.4), various concentrations of the newly synthesized compounds or reference compounds, and adequate amounts of recombinant hMAO-A or hMAO-B. This mixture was incubated for 15 min at 37 °C in a 96-well microplates, placed in the dark fluorimeter chamber. After this incubation period, the reaction was started by adding 200 μM Amplex Red reagent, 1 U/mL horseradish peroxidase (HRP), and *p*-tyramine (concentration range 0.05–1.00 mM).

The production of H₂O₂ catalyzed by MAO isoforms was detected using Amplex®-Red reagent, a non-fluorescent probe that reacts with H₂O₂ in the presence of horse radish peroxidase to produce the fluorescent product resorufin. The reaction was started by adding 200 μM Amplex Red reagent, 1 U/mL horseradish peroxidase, and *p*-tyramine (concentration range 0.1–1 mM). Control experiments were carried out by replacing the compound and reference inhibitors. The possible capacity of compounds to modify the fluorescence generated in the reaction mixture due to non-enzymatic inhibition was determined by adding these compounds to solutions containing only the Amplex Red reagent in a sodium phosphate buffer.

2.3.3. Kinetic experiments

All the synthesized fluorinated methoxylated chalcones were dissolved in dimethyl sulfoxide, with a maximum concentration of 1% and used in the concentration range of 0.01–2.00 μM . The mode of MAO inhibition was examined using Lineweaver-Burk plotting. The slopes of the Lineweaver-Burk plots were plotted versus the inhibitor concentration and the K_i values were determined from the x-axis intercept as $-K_i$. Each K_i value is the representative of single determination where the correlation coefficient (R^2) of the replot of the slopes versus the inhibitor concentrations was at least 0.98. SI was calculated as K_i (hMAO-A)/ K_i (hMAO-B). The protein was determined according to the Bradford method [22].

2.3.4. Reversibility experiments

Reversibility of the MAO inhibition with synthesized compounds was determined by centrifugation-ultrafiltration method previously described [23]. Briefly, adequate amounts of the recombinant enzymes (hMAO-A or B) were incubated with a single concentration of the synthesized compounds or the reference inhibitors in a sodium phosphate buffer (0.05 M, pH 7.4) for one hour at 37 °C. An aliquot was stored at 4 °C and used for the measurement of MAO-A and -B activity. The remaining incubated sample was placed in an Ultrafree-0.5 centrifugal tube with a 30 kDa Biomax membrane and centrifuged at 9000g for 20 min at 4 °C. The enzyme retained in the 30 kDa membrane was resuspended in a sodium phosphate buffer at 4 °C and centrifuged two more times. After the third centrifugation, the enzyme retained in the membrane was resuspended in sodium phosphate buffer (300 mL) and an aliquot of this suspension was used for MAO-A and -B activity determination. Control experiments were performed simultaneously (to determine the 100% MAO activity) by replacing the compounds and standards with appropriate dilutions of the vehicles. The corresponding values of percent (%) MAO isoform inhibition was separately calculated for samples with and without repeated washing.

2.4. Molecular docking methodology

In the current molecular simulation study, AUTODOCK4.2 software was used to establish a ligand-based computer modelling program for the prediction of binding energy of the selected compounds with MAO isoenzymes [24].

2.4.1. Preparation of enzymes

Preparation Wizard of Maestro-8.4 (Schrodinger LLC) has been used to prepare protein. Crystallographic models 2BXR (hMAO-A) and 2BYB (hMAO-B) were downloaded from www.rcsb.org [25]. Initially the PDB files of the enzymes were refined by removing the B-chain and keeping the cofactor FAD. Water and covalently linked ligands were deleted and bond order was corrected for FAD. After assigning charge and protonation state finally energy minimization was done using OPLS2005 force field. PDB written by Maestro for prepared proteins were rewritten by pdb format for AutoDock compatible atom type [26].

2.4.2. Preparation ligands

Ligands were prepared through PRODRG webserver (<http://davapc1.bioch.dundee.ac.uk/cgi-bin/prodrgr>). The structures of the ligands were constructed by using ChemDraw (Cambridge Soft, Massachusetts, USA) and saved in MDL Mol format. This format can be uploaded in the PRODRUG web server and the energy minimized ligand structures were saved in the pdb format for further docking studies [27].

2.4.3. Docking protocol

The receptor grid of both enzymes was developed by using $60 \times 60 \times 60$ grid points in xyz with grid spacing of 0.375 Å and the grid box was centred on N5 atom of FAD (cofactor). The Lamarckian genetic algorithm was applied for all molecular docking simulations. Population size of 300, mutation rate of 0.02 and crossover rate of 0.8 were set as the parameters. Simulations were performed using up to 2.5 million energy evaluations with a uttermost of 27,000 multiplications. Each simulation was performed 50 times, yielding 50 docked conformations. In the automated docking procedure, AutoDock output record the result of docking studies with an extension file 'dlg'. The output file involves many details about the docking regarding the binding energy and inhibition constant of ten conformers used in the respective ligand. From the docking results, the lowest docking energy conformations were also the largest conformational cluster, which was chosen to represent the most favourable binding mode between the ligands and enzymes [28].

3. Result and discussion

3.1. Chemistry

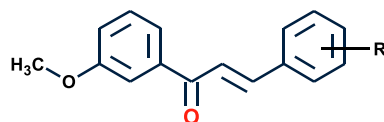
The synthesis of the fluorinated methoxylated chalcones was conducted by the Claisen-Schmidt condensation between 4-methoxyacetophenone with various fluorinated aromatic aldehydes under 40% KOH ethanolic medium. ^1H NMR spectrum showed the peaks of 13 protons compromising of signals of the α - β unsaturated unit, the substituted two phenyl system and methoxyl group. It has been noted that, the up field proton of α carbon and down field proton of β carbon coupled with methine proton with coupling constants (15.6–16.0 Hz). This indicates the presence of trans (*E*) configuration in the fluorinated methoxylated chalcones. A sharp singlet shielded protons in the range of δ 3.908–3.9021 of chalcones strongly recommended the presence of methoxyl group. ^{13}C NMR spectra, the peaks for carbonyl carbon of chalcone and methoxyl group are in the range of δ 188.69–188.18 and 55.49–55.52 respectively. All compounds provided satisfactory elemental analyses.

3.2. Biochemistry

The potential inhibitory activities of the fluorinated methoxylated chalcones on hMAO isozymes were determined by measuring their effects on the production of H_2O_2 from the substrate (p-tyramine), using the Amplex Red MAO assay kit and enzymes (recombinant MAO isoforms). The synthesized compounds did not exhibit any interference with the reagents in the assay medium. The results concerning to hMAO-A and hMAO-B inhibitory activities with the synthesized compounds are presented in Table 1 together with their MAO selectivity indices. The MAO inhibitory activity of chalcone scaffolds has been described previously by different groups and appear to travel along the same style as in the fluorinated methoxylated chalcones. The results demonstrate that these compounds exhibited moderate to good inhibitory activities towards MAO-B than MAO-A. In agreement with the experimental data, all the fluorinated methoxylated chalcones showed productive recognition and selective inhibitory activity towards hMAO-B in the submicromolar range. The following order of MAO inhibitory activity was observed for the fluorinated methoxylated chalcones:

hMAO-A : 2- CF_3 > 3-F > 2-F > 4-F > 4-F₃

hMAO-B : 4- CF_3 > 4-F > 2-F > 3-F > 2- CF_3

Table 1Experimentally determined K_i values for the inhibition of hMAO-A and -B with synthesized fluorinated methoxylated chalcones.

Compounds	R	K_i (MAO-A) (μM) ^a	K_i (MAO-B) (μM) ^a	SI ^b	Inhibition type	Reversibility	Selectivity
M1	2-F	2.34 ± 0.19	0.28 ± 0.02	0.12	Competitive	Reversible	MAO-B
M2	3-F	1.46 ± 0.11	0.35 ± 0.02	0.24	Competitive	Reversible	MAO-B
M3	4-F	2.39 ± 0.20	0.27 ± 0.01	0.12	Competitive	Reversible	MAO-B
M4	2-CF ₃	0.90 ± 0.22	0.36 ± 0.02	0.40	Competitive	Reversible	MAO-B
M5	4-CF ₃	4.32 ± 0.25	0.22 ± 0.01	0.05	Competitive	Reversible	MAO-B
Selegiline	–	8.15 ± 1.33	0.35 ± 0.02	0.04	Suicide	Irreversible	MAO-B
Moclobemide	–	0.010 ± 0.002	1.45 ± 0.04	140.0	Competitive	Reversible	MAO-A

^a Each value represents the mean ± SEM of three independent experiments.^b The selectivity index (SI) was calculated as K_i (MAO-B)/ K_i (MAO-A).

All the fluorinated chalcones exhibited good activity in the submicromolar range towards MAO-B, but among them the highest activity was observed for the methoxylated chalcones that were substituted with a trifluoromethyl group in the 4-position of the B ring. Our data revealed that the newly synthesized compounds exhibited strong and selective inhibitory activity against hMAO-B. Among these five compounds, **M5** showed the best activity and higher selectivity towards hMAO-B with K_i and SI values of $0.22 \pm 0.01 \mu\text{M}$ and 0.05, respectively, surpassing that of selegiline, the reference selective and irreversible MAO-B inhibitor (K_i and SI values were found as $0.33 \pm 0.03 \mu\text{M}$ and 0.04, respectively). Based on high inhibition potency and MAO-B selectivity as selection criteria, **M5** was considered a promising lead compound for the development of reversible MAO-B inhibitors. Compounds **M3** and **M1** were also found to be a potent MAO-B inhibitor with a K_i value of 0.27 and 0.28 μM respectively. Substitution of both trifluoromethyl and fluoro group in the para position of the B ring of methoxylated chalcone enhances the MAO-B inhibition potencies with greater extent. The results also demonstrate that the increasing the bulkiness with addition of trimethyl group in the para position of ring B in methoxylated chalcones favours the activity ratio towards MAO-B. A logical explanation for this observation is that the higher degree of lipophilicity of the trifluoromethyl group compared with the fluorine atom facilitates more productive Van der Waals interactions with the inhibitor binding cavity of MAO-B.

Kinetic analyses were carried out for most potent MAO-B inhibitor **M5** from this series. The aim of this experiment was to find the mode of MAO-B inhibition by fluorinated methoxylated chalcones. A set of Lineweaver-Burke plots were constructed in the absence and presence of various concentrations of compound **M5**. The observation that the lines were linear and intersect on the y-axis suggests that **M5** interacts with the catalytic site of hMAO-B, with a competitive mode of inhibition. (Fig. 3). The replots of the slopes of the Lineweaver–Burk plots versus inhibitor concentration is shown in Fig. 4 and the K_i was estimated as 0.22 μM for **M5**. In the reversibility and irreversibility tests, hMAO-B inhibition was found to be reversible in presence of the compounds as shown by the recovery enzyme activity after repeated washing. Table 2 presents the reversibility of hMAO-B inhibition with the chalcone compounds. Reversibility of hMAO-B inhibition with compound **M5** was found to be good in this series. The percentage inhibition (%) of hMAO-B of compound **M5** (0.5 μM) was calculated as 86.90 ± 6.33 and 11.02 ± 0.10 before and after washing, respectively.

Another interesting aspect is the inhibitory capacity **M4** compound which showed K_i value of 0.36 and 0.90 μM towards both MAO-B and A respectively. It is to be noted that dual-target-directed MAO-A and B inhibitors may have enhanced therapeutic value, making such compounds ideal adjuvants to L-Dopa treatment in Parkinson's disease, particularly when

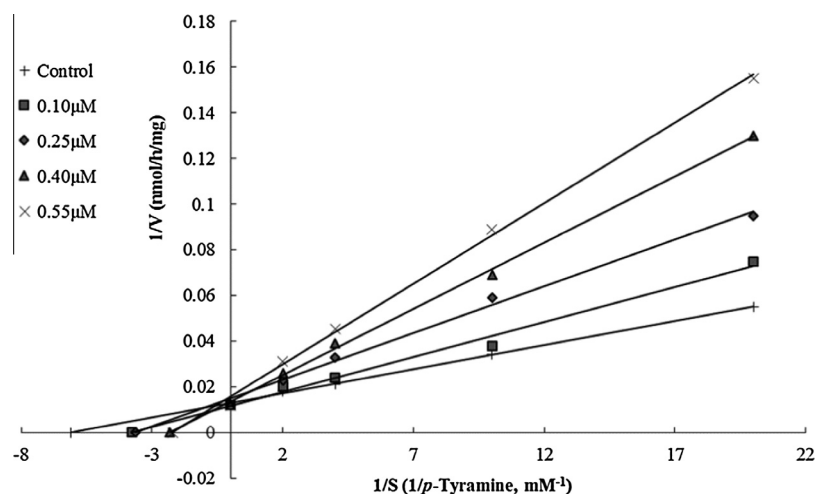


Fig. 3. Lineweaver–Burk plots of the oxidation of p-tyramine by recombinant hMAO-B. The plots were constructed in the absence and presence of various concentrations of compound (0.10–1.50 μM) **M5**.

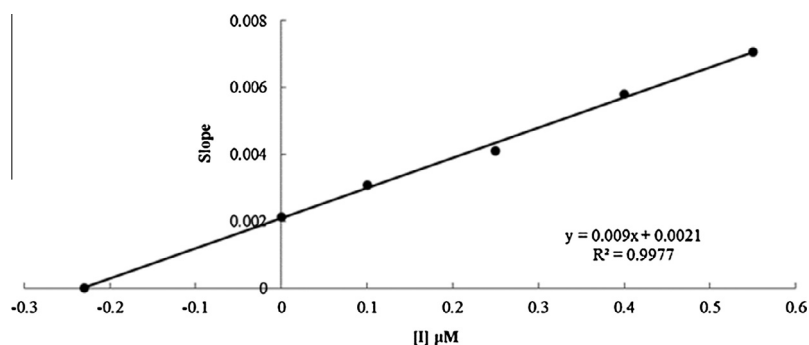


Fig. 4. Replots of the slopes of the Lineweaver–Burk plots versus inhibitor (**M5**) concentration.

Table 2

Reversibility of hMAO-B inhibition the newly synthesized fluorinated methoxylated chalcones.

Compound (50 μM)	hMAO-B inhibition (%)	
	Before washing	After repeated washing
Selegiline	47.09 \pm 3.25	46.38 \pm 3.10
M1	82.46 \pm 6.03	14.21 \pm 1.20
M2	80.24 \pm 5.67	15.00 \pm 1.18
M3	83.00 \pm 6.05	13.90 \pm 1.05
M4	77.75 \pm 5.00	17.18 \pm 1.30
M5	86.90 \pm 6.33	11.02 \pm 0.10

Each value represents the mean \pm SEM of three experiments.

associated with depression [29]. Thus, besides deriving additional SARs for the inhibition of the chalcone type MAOs and potentially discovering highly potent MAO-B inhibitors, this study will also facilitate the comparison of the MAO-B inhibition properties of fluorine and the trifluoromethyl group in the various positions of the **B** ring of chalcones.

3.3. Molecular docking studies

Molecular docking studies were carried out to further explain the *in vitro* results of the new compounds, and to identify the hypothetical binding mode for the compounds inside the inhibitor binding cavity of hMAO-A and B. Molecular docking scores and the calculated inhibition constants towards both MAO-A and MAO-B of titled derivatives were shown in Table 3. Experimental data concerning the hMAO inhibitory activities of fluorinated methoxylated chalcones were found to be in a good agreement with the calculated data obtained from the molecular docking studies (Figs. 5 and 6). The inhibitor binding cavity of MAO-B is characterized by two large pockets. Pocket 1 involves, a large aromatic cage made up of FAD, Phe 343 and four tyrosine residues Tyr 188, 189, 435 and 398. Pocket 2 a hydrophobic pocket characterized by Leu 171, Tyr 326, Phe 168, Ile 198 and 199. Here smaller entrance cavity' with Ile 199 effectively serves as a gate between these cavities [30]. Depending on the structure of the bound inhibitor the two cavities may be either separate or fused [31].

The docking studies of **M5** reveals that the p-methoxyl group in the **A** ring of chalcone is positioned between the phenolic side

Table 3

Theoretically determined binding energy and K_i values of the newly synthesized fluorinated thienylchalcones for the inhibition of hMAO-A and -B.

Si No.	Code	MW	Binding energy for MAO-A (kcal/mol)	Binding energy for MAO-B (kcal/mol)	Calculated K_i value for MAO-A (μM)	Calculated K_i value for MAO-B (μM)	Calculated SI^*
1.	M1	256.27	-7.78	-8.74	2.00	0.39	0.19
2.	M2	256.27	-7.97	-8.78	1.43	0.37	0.25
3.	M3	256.27	-7.76	-8.81	2.06	0.35	0.16
4.	M4	306.28	-8.36	-8.78	0.75	0.37	0.49
5.	M5	306.28	-7.61	-8.71	2.66	0.42	0.15

* Molecular weight.

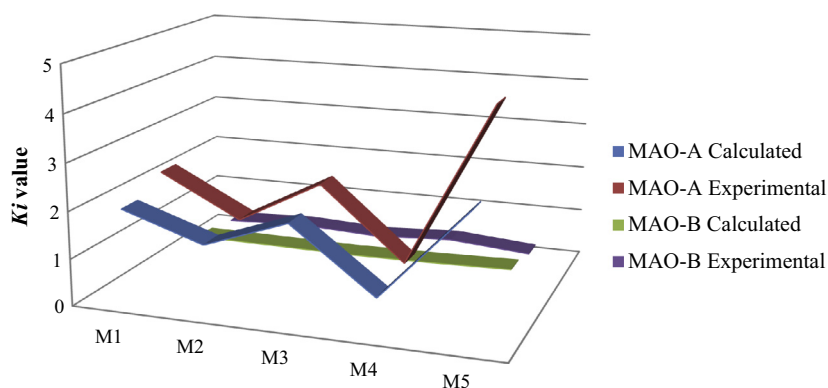


Fig. 5. Experimental and calculated K_i values corresponding to the inhibition of hMAO-A and -B with **M** series compounds.

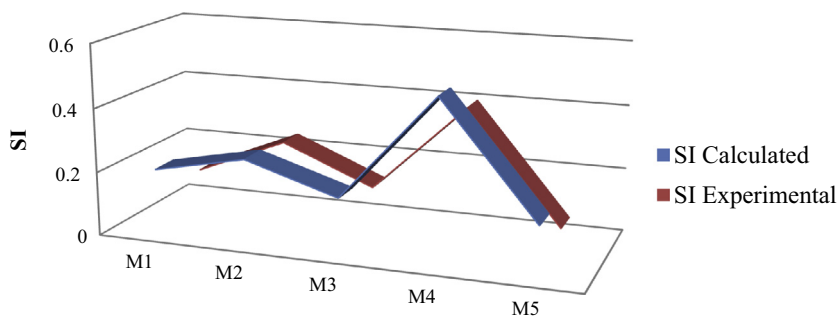


Fig. 6. Experimental and calculated selectivity indices (calculated as K_i (MAO-B)/ K_i (MAO-A)) for the **M** series towards hMAO isoforms.

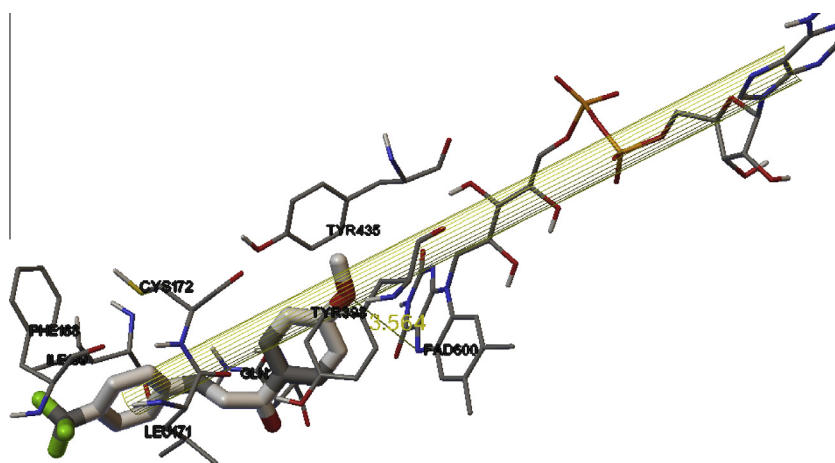


Fig. 7. Docking picture of **M5** in the MAO-B active site.

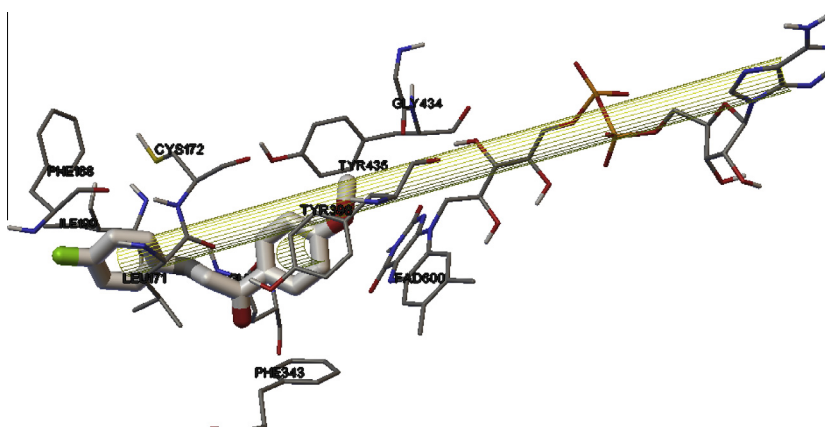


Fig. 8. Docking picture of **M3** in the MAO-B active site: Yellow mesh indicates π - π stacking interaction.

chains of Tyr398 and Tyr435 MAO-B and is anchoring from the *re face* of FAD with a distance of 3.564 Å (Fig. 7). This interaction is mainly stabilized by the strong π - π interaction between **B** ring of the **M5** and the FAD unit. The strong electron withdrawing trifluoromethyl group in the para position of the **B** ring of the methoxylated chalcone significantly reduces the electron density and is capable of forming more π - π stacking interaction with aromatic cages of the inhibitor binding cavity of MAO-B [32]. This stabilizing

interaction of the fluorinated methoxylated chalcones showed good proximity towards the isoalloxazine of FAD unit. The potent inhibitor **M3** also showed a similar type of interactions like **M5** in the inhibitor binding cavity of MAO-B (Fig. 8). From the close inspection of docking pose of **M3**, fluorine atom in the **B** ring of chalcone lined with the entrance cavity of Ile199 and the methoxyl group was positioned between the Tyr435 and Tyr 396 in the aromatic cage and is anchoring from the *re face* of FAD. **M3** is mainly

stabilized by the strong π - π interaction of FAD unit and Tyr398 of **B** and **A** ring respectively. As mentioned above, the trifluoromethyl and the fluorine groups of the **M5** and **M3** of **B** ring are located within the entrance cavity of MAO-B since it is a hydrophobic environment [33].

The presence trifluoromethyl and the fluorine groups in the **B** ring of chalcones are stabilized to a large degree by Van der Waals interactions within the entrance cavity of Ile199. Therefore, substitution with halogens on the chalcone system is expected to enhance the productive interactions of the inhibitor with the entrance cavity of MAO-B via hydrophobic burial and dipole interactions. The enhancement of MAO-B inhibition potencies by halogen substitution has been previously described. For example, chlorine and bromine substitution on the benzyloxy phenyl ring of a series of 8-benzyloxycaffeinines enhances the MAO-B inhibition potencies 20 and 22-fold, respectively [34].

4. Conclusion

The study mainly highlights the effect and orientation of fluorine and the trifluoromethyl group in the **B** ring of a methoxylated chalcones towards MAO inhibition. The results document that all the chalcone derived compounds showed potent MAO-B inhibitory activity in the submicromolar range. Compound **M5** is not simply a high potent MAO-B inhibitor, but also revealed relatively good selectivity for MAO-B over the MAO-A isoform. The study revealed the importance of lipophilic halogen groups in the para position of the **B** ring of chalcone compounds and is promising for the development of new selective and reversible type of MAO-B inhibitors. It may thus be concluded that **M5** is a promising lead for the development of reversible and selective MAO-B inhibitors, which can be used in the treatment of Parkinson's disease. To our best knowledge, this is the first report on the MAO inhibition activity of fluorinated methoxylated chalcones. Further structural optimization and the modification of this scaffold are well under way in our laboratory.

Acknowledgment

The authors extend their appreciation to Kerala State Council for Science, Technology & Environment, Kerala, India (application no: 01/SPS-54/2015/CSTE) for the financial support. The authors also thankful to IIRBS, Mahatma Gandhi University, Kottayam, India for carrying out the spectral analysis.

Appendix A. Supplementary material

Supplementary data associated with this article can be found, in the online version, at <http://dx.doi.org/10.1016/j.bioorg.2015.07.001>.

References

- [1] M. Yáñez, J.F. Padín, J.A. Arranz-Tagarro, M. Camiña, R. Laguna, *Curr. Top. Med. Chem.* 12 (2012) 2275–2282.
- [2] M.B.I. Youdim, Y.S. Bakhle, *Br. J. Pharmacol.* 147 (2006) S287–S296.
- [3] L. Oreland, S.S. Jossan, P. Hartvig, S.M. Aquilonius, B. Langstrom, *J. Neural. Transm. Suppl.* 32 (1990) 55–59.
- [4] J. Reis, I. Encarnaçao, A. Gaspar, A. Morales, N. Milhazes, F. Borges, *Curr. Top. Med. Chem.* 12 (2012). 2177–2118.
- [5] H.H. Fernandez, J.J. Chen, *Pharmacotherapy* 27 (2007) 1745–1855.
- [6] G. Di Carlo, N. Mascolo, A.A. Izzo, F. Capasso, *Life Sci.* 65 (1999) 337–353.
- [7] O. Afzal, S. Bawa, S. Kumar, R. Kumar, Md.Q. Hassan, *Lett. Drug Des. Discov.* 10 (2013) 75–85.
- [8] S. Tanaka, Y. Kuwai, M. Tabata, *Planta Med.* 53 (1987) 5–8.
- [9] T. Hatano, T. Fukuda, T. Miyase, T. Noro, T. Okuda, *Chem. Pharm. Bull.* 39 (1991) 1238–1243.
- [10] X. Pan, L.D. Kong, Y. Zhang, C.H. Cheng, R.X. Tan, *Acta Pharmacol. Sinica* 21 (2000) 949–953.
- [11] H. Haraguchi, Y. Tanaka, A. Kabbash, T. Fujioka, T. Ishizu, A. Yagi, *Phytochemistry* 65 (2004) 2255–2260.
- [12] F. Chimenti, R. Fioravanti, A. Bolasco, P. Chimenti, D. Secci, F. Rossi, M. Yanez, F. Orallo, F. Ortuso, S. Alcaro, *J. Med. Chem.* 52 (2009) 2818–2824.
- [13] G. Jo, S. Ahn, B.G. Kim, H.R. Park, Y.H. Kim, A.H. Cho, D. Koh, Y. Chong, J.H. Ahn, Y. Lim, *Biorg. Med. Chem.* 21 (2013) 7890–7897.
- [14] S.J. Robinson, J.P. Petzer, A. Petzer, J.J. Bergh, A.C.U. Lourens, *Bioorg. Med. Chem. Lett.* 23 (2013) 4985–4989.
- [15] B. Evranos-Aksöz, S. Yabanoglu-Çiftçi, G. Uçar, K. Yelekcı, R. Ertan, *Bioorg. Med. Chem. Lett.* 24 (2014) 3278–3284.
- [16] N. Morales-Camilo, C.O. Salas, C. Sanhueza, C. Espinosa-Bustos, S. Sepúlveda-Boza, M. Reyes-Parada, F. Gonzalez-Nilo, M. Caroli-Rezende, A. Fierro, *Chem. Biol. Drug Des.* 85 (2015) 685–695.
- [17] A.M. Helguera, G. Pérez-Machado, M.N.D.S. Cordeiro, F. Borges, *Mini Rev. Med. Chem.* 12 (2012) 907–919.
- [18] B.V. Nayak, S. Ciftci-Yabanoglu, S. Bhakat, A.K. Timiri, B.N. Sinha, G. Ucar, M.E.S. Soliman, V. Jayaprakash, *Bioorg. Chem.* 58 (2015) 72–80.
- [19] M.C. Anderson, F. Hasan, J.M. McCrodden, K.F. Tipton, *Neurochem. Res.* 18 (1993) 1145–1149.
- [20] F. Chimenti, E. Maccioni, D. Secci, A. Bolasco, P. Chimenti, A. Granese, S. Carradori, S. Alcaro, F. Ortuso, M. Yáñez, *J. Med. Chem.* 51 (2008) 4874–4880.
- [21] M. Yáñez, N. Fraiz, E. Cano, F. Orallo, *Biochem. Biophys. Res. Commun.* 344 (2) (2006) 688–695.
- [22] M.M. Bradford, *Anal. Biochem.* 72 (1976) 248–254.
- [23] F. Chimenti, S. Carradori, D. Secci, A. Bolasco, B. Bizzarri, P. Chimenti, A. Granese, M. Yáñez, F. Orallo, *Eur. J. Med. Chem.* 45 (2010) 800–804.
- [24] G.M. Morris, R. Huey, W. Lindstrom, M.F. Sanner, R.K. Belew, D.S. Goodsell, A.J. Olson, *J. Comput. Chem.* 30 (2009) 2785–2791.
- [25] L. De Colibus, M. Li, C. Binda, A. Lustig, D.E. Edmondson, A. Mattevi, *Proc. Natl. Acad. Sci. USA* 102 (36) (2005) 12684–12689.
- [26] B.V. Nayak, S. Ciftci-Yabanoglu, S.S. Jadav, M. Jagrat, B.N. Sinha, G. Ucar, V. Jayaprakash, *Eur. J. Med. Chem.* 69 (2013) 762–767.
- [27] A.W. Schuttelkopf, D.M. van Aalten, *Acta Crystallogr. D Biol. Crystallogr.* 60 (2004) 1355–1363.
- [28] B. Mathew, J. Suresh, S. Anbazhagan, S. Dev, *Biomed. Aging Pathol.* 4 (2014) 297–301.
- [29] L.J. Legoabe, A. Petzer, J.P. Petzer, *Chem. Biol. Drug Des.* (2015), <http://dx.doi.org/10.1111/cbdd.12508>.
- [30] C. Binda, M. Li, F. Hubalek, N. Restelli, D.E. Edmondson, *Proc. Natl. Acad. Sci. USA* 100 (2003) 9750–9755.
- [31] L. Legoabe, J. Kruger, A. Petzer, J.J. Bergh, J.P. Petzer, *Eur. J. Med. Chem.* 46 (2011) 5162–5174.
- [32] D.E. Edmondson, A. Mattevi, C. Binda, M. Li, F. Hubalek, *Curr. Med. Chem.* 11 (2004) 1983–1993.
- [33] L. Novaroli, A. Daina, E. Favre, J. Bravo, A. Carotti, F. Leonetti, M. Catto, P.A. Carrupt, M. Reist, *J. Med. Chem.* 49 (2006) 6264–6272.
- [34] B. Strydom, S.F. Malan Jr., N. Castagnoli, J.J. Bergh, J.P. Petzer, *Bioorg. Med. Chem.* 18 (2010) 1018–1028.